

Identifying recharge and salinization sources of groundwater in the Oussja Ghar el Melah plain (northeast Tunisia) using geochemical tools and environmental isotopes

Safouan Ben Ammar^{1,3} · Jean-Denis Taupin² · Kamel Zouari³ · Mohamed Khouatmia⁴

Received: 13 August 2015 / Accepted: 2 February 2016 / Published online: 31 March 2016
© Springer-Verlag Berlin Heidelberg 2016

Abstract The recharge sources and groundwater degradation in the coastal plain of Oussja Ghar el Melah were investigated using geochemical and isotopes tools. We demonstrate that the water quality of shallow groundwater in the phreatic aquifer is impacted by long-term intensive irrigation. We show that the factors controlling the salinity and composition of groundwater are the return flow of the irrigation water, the water–rock interaction in the aquifer and salts formed on the surface by marine sprays. In the low plain where NO_3^- content is of up to about 140 mg/L, groundwater is affected by diffuse pollution caused by intensive agricultural activities. In the upstream part of the plain and in the area situated in the SW, stable isotopes and tritium values indicate recent recharge by local precipitation.

Keywords Coastal aquifer · Groundwater · Hydrogeochemistry · Water isotopes · Ghar el Melah · Tunisia

Introduction

Coastal areas in the Mediterranean basin are characterized by large water demand, caused by continuous growth in population, intensive agricultural practices and developing of industrial and touristic activities. Intensive exploitation of coastal aquifers to satisfy the important demand especially for domestic and agriculture uses may generate problems due to resources scarcity, quality degradation and marine intrusion (Barale and Folving 1996; Custodio and Bruggeman 1987; Ma et al. 2007; Custodio 2010). The most severe problems related to groundwater quality in these areas are rapid salinization of water resources and nitrate pollution. A combination of natural causes (low aquifers recharge due to low and variable precipitation) and anthropogenic factors (high water demand and wide fertilizer use caused by intensive agriculture practice, extension of urban areas, wastewater use in irrigation, etc.), have caused significant water quality degradation in the last few decades (Stigter et al. 1998; Re and Zuppi 2011).

The abundance of water, the fertility of the soil and mild climate in eastern coastal plains of Tunisia have induced continued migration to these areas (75 % of the Tunisian population live in coastal cities). As a consequence to the population progressive growth and the increasing of economic and touristic activities, the demand for water is increasing progressively. Intensive pumping of groundwater for several years, with concomitantly increasing in agricultural activities has led to qualitative and quantitative degradation of groundwater resources. Declining of groundwater level, excessive salinization of water resources and sea water

✉ Safouan Ben Ammar
safouan_ammarr@yahoo.fr

Jean-Denis Taupin
taupin@msem.univ-montp2.fr

Kamel Zouari
kamel.zouari@enis.rnu.tn

Mohamed Khouatmia
mh_khouatmia@yahoo.fr

¹ Institut Supérieur des Technologies de l'Environnement de l'Urbanisme et de Bâtiment (ISTEUB), La Charguia II, Univ. Carthage, 2 Rue de l'Artisanat Charguia 2, 2035 Tunis, Tunisia

² Hydrosociences, UMR 5569 (IRD, CNRS, UM1, UM2), Montpellier, France

³ LRAE, ENI Sfax, Univ. Sfax, route de Soukra, Sfax, Tunisia

⁴ CNSTN, Sidi Thabet, Tunis, Tunisia

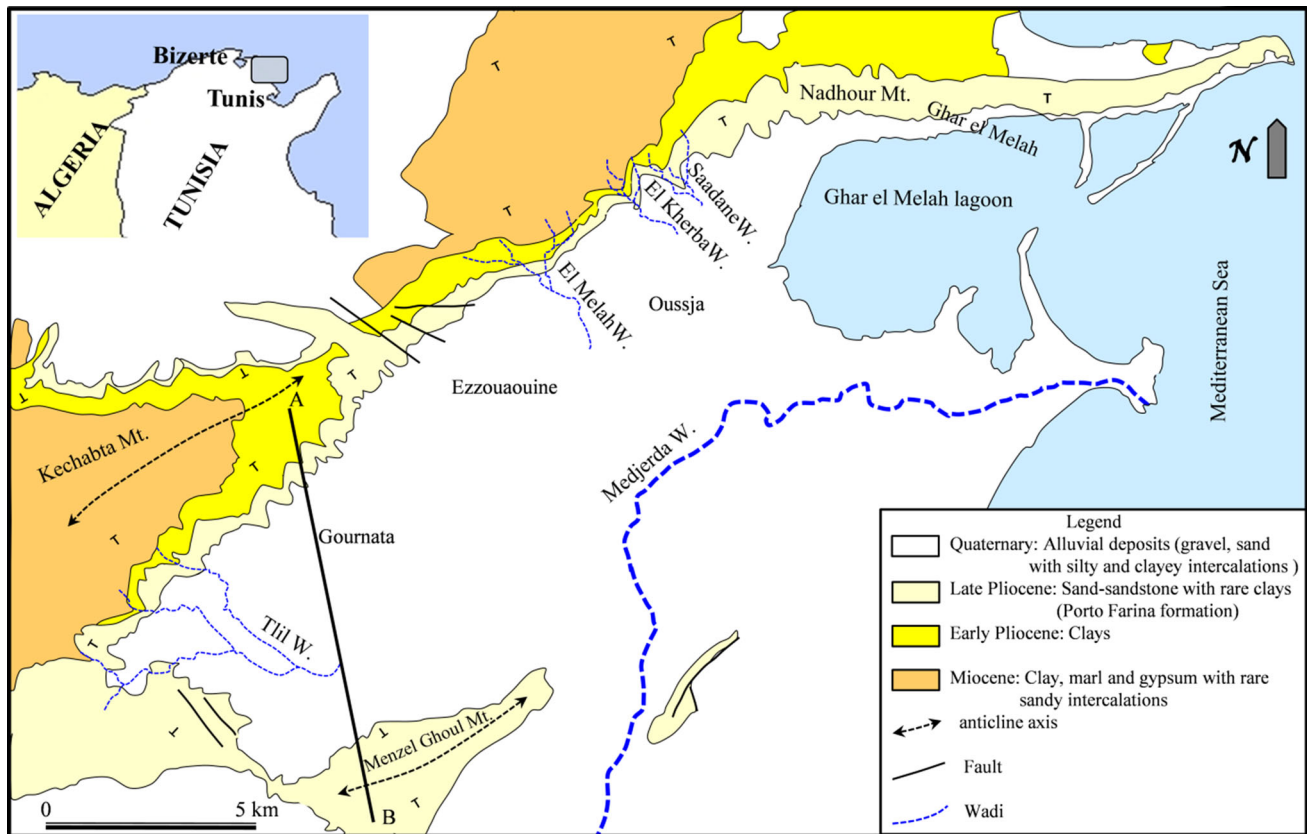


Fig. 1 Geological and location map of the study area (Burrolet and Dumon 1952; Melki et al. 2011). Line AB is the location of the geological cross section presented in Fig. 2

intrusion are the common results of increase in groundwater abstraction observed in recent years (e.g., Fedrigoni et al. 2001; Trabelsi et al. 2007; Kouzana et al. 2009).

The plain of Oussja Ghar el Melah (OGM) is an example of the largest agricultural production area in the NE part of Tunisia. Groundwater from the shallow aquifer provides almost all water supply for irrigation. For many years ago, the growth over time of agricultural activities, has led to an ever-rising increase in water demand. Intensive groundwater exploitation, carried out without careful planning, has, however, brought about severe deterioration of water resources.

In the present study, environmental isotopes (^{18}O , ^2H and ^3H) in conjunction with hydrochemistry (major ions and Br^-) were employed to understand the groundwater recharge process and to determine sources of quality deterioration under the influence of intensive agricultural activities in the coastal plain of Oussja Ghar el Melah.

Geological setting

The OGM plain (135 km²) is located in the NE part of Tunisia. It is bounded on the north and in west sides by mountainous relief: Nadhour Mountain in the north

(300 m) and Kechabta Mountain in the west (400 m). In the east, the boundary is formed by the Mediterranean Sea and by the Wadi of Medjerda and Menzel Ghoul Mountain in the South (Fig. 1).

The study area is a part of the molasse basin related to the major subsidence period during the Mio-Pliocene. Miocene formations represented by clay, marl and gypsum alternating with rare sandy intercalations are the oldest rocks outcropping in the surrounding mountains of the study area (Burrolet and Dumon 1952; Melki et al. 2011). These formations are covered by clay sequences attributed to Early Pliocene (Fig. 1). A thick Upper Pliocene formation (Porto Farina formation) made of sand and sandstone with clays intercalations overlies the impervious clay layers of Miocene and Late Pliocene (Chelbi et al. 1995; Oueslati et al. 2006; Mejri et al. 2010; Melki et al. 2011; Mejri 2012). The thickness of the Porto Farina formation is about 300 m (Burrolet and Dumon 1952; Melki et al. 2011). As Menzel Ghoul mountain situated in SW part of the study area, Nadhour and Kechabta mountains correspond to anticlines structures continuing in the south with a syncline structure forming the OGM plain (Figs. 1, 2). This depression constitutes the old delta of Medjerda. The plain was historically occupied by the Ghar el Melah lagoon

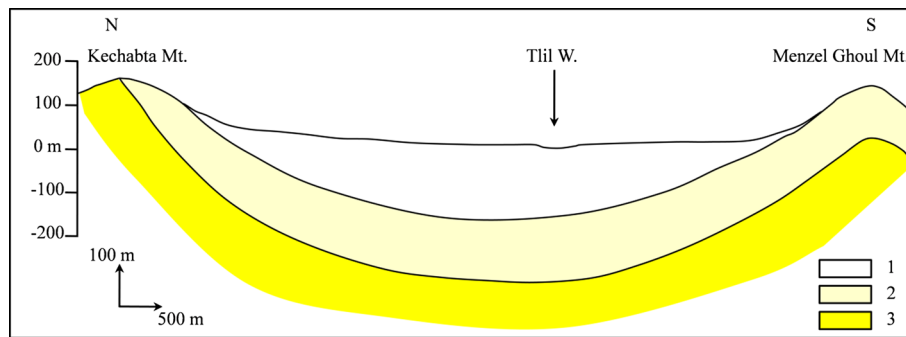


Fig. 2 Simplified geologic cross section in the plain of OGM. 1 Quaternary (fluvial deposits), 2 late Pliocene (sand and sandstone of Porto Farina formation), 3 early Pliocene (clays)

(5000 years ago) and then filled with recent fluvial deposits composed of alternation of sand, silt and clay attributed to Holocene period (Burrolet and Dumon 1952; Oueslati et al. 2006). The thick sequence formed by Upper Pliocene and Quaternary deposits hosts the OGM phreatic aquifer. Seismic reflection study carried out in the studied area (Melki et al. 2011) shows that the thickness of the Plio-Quaternary formations varies from 300 m in the SW part of the plain (Gournata) to more than 600 m in the East part (between Oussja and the lagoon of Ghar el Melah).

The plain is characterized by low altitudes that rarely exceed 20 m in the foot of the mountains and are close to 3 m in the central part of the plain. These low topographic slopes favored the extension of wet and marshy lands in the eastern part around the Wadi Medjerda and in the west of the lagoon of Ghar el Melah.

Climatic and hydrogeological settings

The study area is characterized by a semi-arid climate with approximately 500 mm of mean annual precipitation, with the majority of precipitation occurring during the winter months between October and April (90 %). The mean annual temperature is of 18.8 °C with a minimum of 11.3 °C in February and a maximum of 26.8 °C in August. As estimated by means of empirical formula such as those of Thornthwaite, Turc, and Penman The mean annual ETP is of 1346 mm/year.

The plain of OGM corresponds to a depression (syncline structure) filled by recent Plio-Quaternary heterogeneous alluvial deposits represented essentially by sands, silts and clays. These sediments that have locally high infiltration capacity constitute the phreatic aquifer in the plain. This coastal aquifer is recharged by water flowing from the surrounding hills, where Plio-Quaternary sediments outcrop, as well as by local infiltration on the plain (central and downstream part) and from the different rivers crossing the plain: Wadi Saadane and el Kherba in

the north, wadi el Melah in the central part and Wadi Tlil in the south–west.

Groundwater flow determined from well records is from the NW to SE, where it discharges to the Ghar el Melah lagoon and to the wet lands (called Sebkhha) crossed by Wadi Medjerda (Fig. 3). The static water level varies between about 60 and 70 m below the ground in the northwestern areas near the mountains to less than 1 m in the downstream part of the plain around the Ghar el Melah lagoon. Pumping tests showed low transmissivity values varying from 3 to $9 \times 10^{-4} \text{ m}^2/\text{s}$ in SW part (Gournata) to 1 to $5.5 \times 10^{-4} \text{ m}^2/\text{s}$ in the central part of the plain (Oussja).

In the plain of OGM the groundwater is used essentially for irrigation. Groundwater abstraction is about 13 millions m^3 by the means of 1450 hand-dug wells (about 11 wells/ km^2) equipped with pumps.

During recent decades, the phreatic aquifer of OGM, suffers from an excessive exploitation due to an increase in water demand to satisfy agriculture sector and to the extension of cultivated lands. Pumped groundwater reaching 13 millions m^3 in 2009 is superior to estimated resources (7 millions m^3). As shown in the piezometric contour map (Fig. 3), there is no severe drawdown of the piezometric levels observed near the sea. In the current state of knowledge, the overexploitation of groundwater resources seems not affecting the hydrodynamic of the water table and there is no seawater intrusion process declared. The anthropic effect caused by intensive pumping for irrigation in the dry season (from May to August) is offset by an excess in precipitation and limitation of pumping in the rainy season from October to April.

Methods

Sixty three samples (including Mediterranean Sea water, Ghar el Melah lagoon water and one spring: sample number 10) were collected for geochemical analysis (major

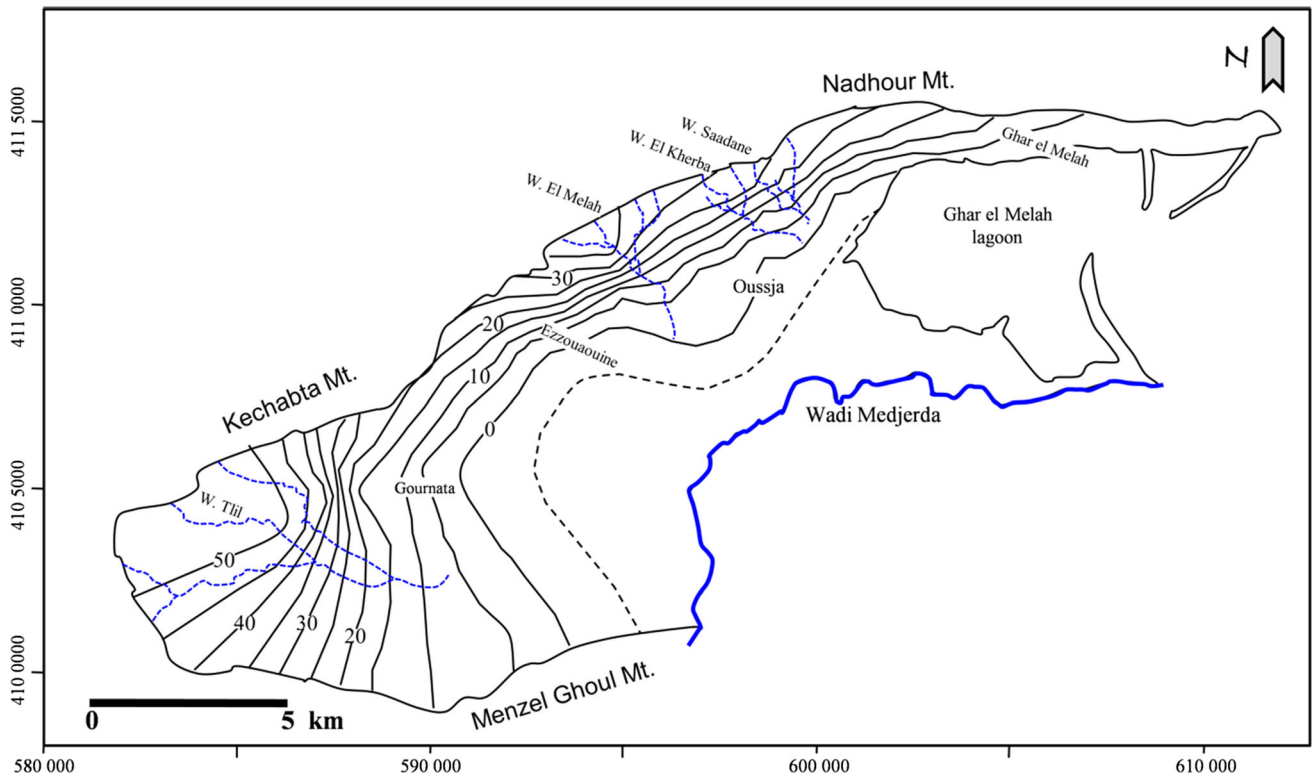


Fig. 3 Piezometric contour map of the study area

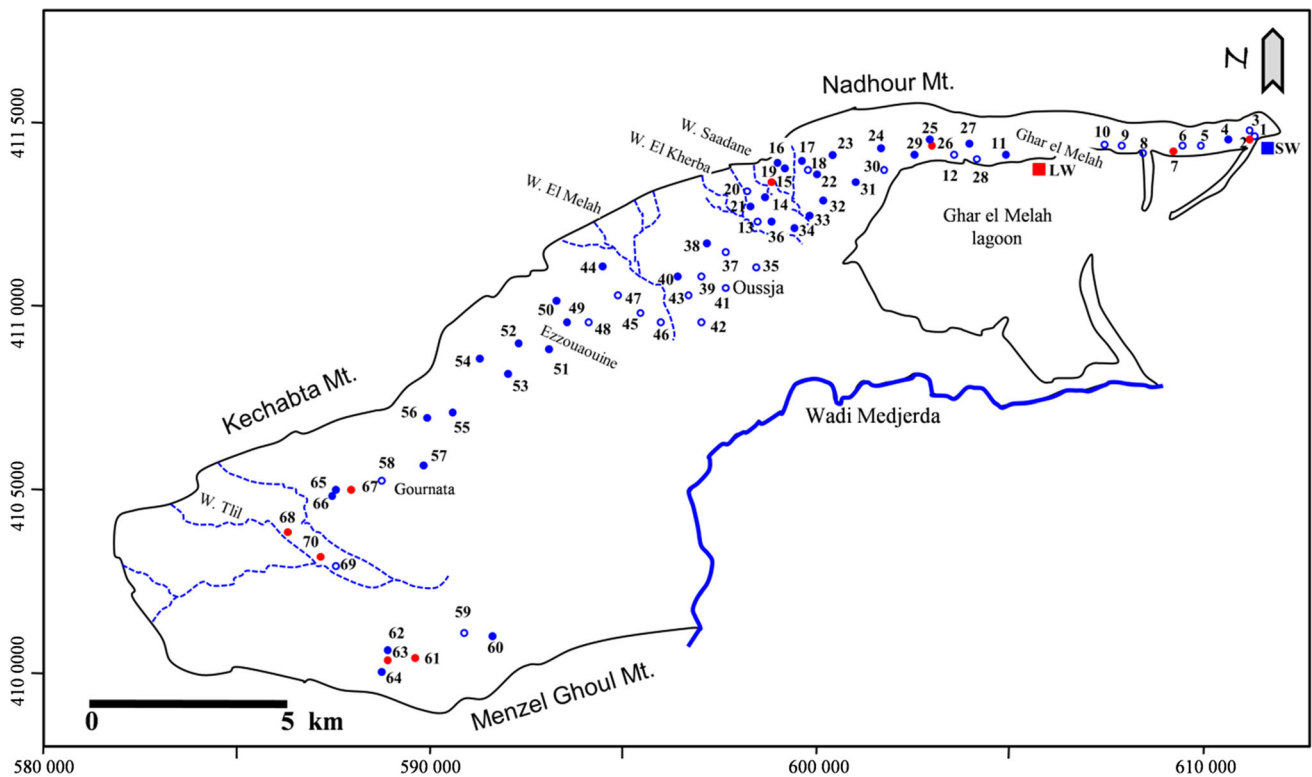


Fig. 4 Location of sampled wells in the study area. *Blue circles* Sampled wells for geochemical and isotope study (*open circles* Cl^- - Na^+ water type, *closed circles* Cl^- - Na^+ / Ca^{2+} water type), *red circles*

well used only for piezometric measurements, *blue square* sea water (SW), *red square* lagoon water (LW)

elements) and isotopes (^2H , ^{18}O and ^3H) between March and May 2010 (Fig. 4). Well locations were chosen to achieve a diverse spatial representation with different depths. The static water level in sampled wells varies from 0.5 to 59.5 m below the ground surface. Samples were collected from pumped wells in a polyethylene bottles. All samples for chemical analyses were filtered in the field through 0.45 μm filters to remove all suspended solids.

Chemical analyses were done with ion chromatography method in the National Centre for Nuclear Sciences and Technology (CNSTN) using a Dionex DX120 ion chromatograph. The precision and accuracy of analyses based on the electro-neutrality of samples were better than 5 %. Electrical conductivity (EC), temperature and pH were measured in situ.

Samples for stable isotope analysis were collected according to the procedures described by Clark and Fritz (1997). Stable isotopes were carried out on an Isoprime–GV Instruments mass spectrometer in the LAMA (Montpellier—France). Hydrogen isotope composition was measured by water reduction over metallic chrome, while $\delta^{18}\text{O}$ was analyzed by water- CO_2 equilibration; both results are expressed in δ ‰ V-SMOW (IAEA 1995) with an overall precision of 0.05 ‰ for ^{18}O and 0.8 ‰ for ^2H . Tritium concentration was determined by a scintillation counter following electrolytic enrichment in the LRAE–Sfax. The concentrations are expressed as tritium units (TU). Analytical uncertainty of tritium analyses was ± 0.4 TU.

Results

The hydrochemical and isotopes results for groundwater samples from the OGM plain are shown in Table 1. The pH values range from 7 to 8.9 with a neutral average value of 7.5. Independently of well characteristics (depth, geographic situation) the temperatures measured in the field show homogeneous values varying from 15 to 22.8 °C. They seem to be influenced only by the surface air temperature.

The hydrochemical data show that fresh groundwater zones are mainly in the upstream part of the basin (piedmont of mountains) and the SW area influenced by wadi Tlil. In these regions the EC is less than 3.5 mS/cm. The EC increases (EC >3.5 mS/cm) in the lower alluvial plain with the proximity of the wells to the sea and Ghar el Melah lagoon (Fig. 5).

A wide range of salinities and chemical compositions characterize the study area. The TDS values vary between 710 and 5150 mg/L. The correlations established between the TDS and concentrations of major elements (Table 2) show that the TDS is well correlated with the

concentrations of chloride and sodium (respective $r^2 = 0.96$ and 0.91). This correlation reflects the contribution of these elements to the mineralization of groundwater in the studied area. The TDS is also correlated with Br^- ($r^2 = 0.88$) that is in good correlation with Cl^- ($r^2 = 0.93$). A very large variability was also found in the nitrate concentrations, ranging from 4.51 to 136 mg/L.

The Piper diagram (Fig. 6) illustrates two chemical facies that directly related to the nature of the aquifer and the proximity of the sampled wells from the sea. Groundwater is of a $\text{Cl}^- \text{Na}^+/\text{Ca}^{2+}$ type in the border of the basin and in the region situated in the west of Gournata (Fig. 4). In these areas, the aquifer is made of gravel and sandy formations. In the downstream part of the plain near the Ghar el Melah lagoon and the sea, the groundwater is of $\text{Cl}^- \text{Na}^+$ type.

Saturation index (SI) calculation using PHREEQC indicate that the groundwater is saturated with respect to carbonate minerals (calcite, aragonite and dolomite) and unsaturated with respect to evaporated minerals (gypsum and anhydrite).

Groundwater samples show isotopic content ranging from -5.66 to -2.97 ‰ vs V-SMOW for $\delta^{18}\text{O}$ and from -32.3 to -19.1 ‰ vs V-SMOW for $\delta^2\text{H}$. The mean values are, respectively, -4.66 and -28.1 ‰ vs V-SMOW for $\delta^{18}\text{O}$ and $\delta^2\text{H}$. Compared to values measured in the Tunis station (situated at 30 km in the south) (IAEA/GNIP; Celle-Jeanton et al. 2001) stable isotopes content and the tritium data (ranging from 0.4 to 5.1 TU) advocate for a recent groundwater renewal with two different recharge modes: (1) fast recharge due to the infiltration of irrigation water and runoff water through the Plio-Quaternary formation in the plain, and (2) diffuse recharge by direct infiltration of precipitation in the upstream part of the plain where oxygene-18 values decrease with depth (between 15 and 40 m) and groundwater shows a low tritium levels indicating different recharge timing.

Discussion

Groundwater salinization and degradation in coastal areas around the Mediterranean basin is one of the most problems related to groundwater resources treated by several studies recent years (Custodio and Bruggeman 1987; Custodio 2010; Re and Zuppi 2011; Fedrigoni et al. 2001; Trabelsi et al. 2007; Fukada et al. 2004; Kass et al. 2005; Grassi and Cortecchi 2005; Grassi et al. 2007). Salinization is generally related to: (1) seawater intrusion caused by overexploitation of resources, (2) return of irrigation water due to intensive irrigation and low depth of the water table and (3) intensive use of fertilizers by farmers to increase crop productivity.

Table 1 Chemical and isotopic data from sampled wells in the OGM plain

Well	Alt. (M.a.s.l)	SL (m/ground surface)	Depth (m/ground surface)	pH	T (°C)	EC (MS/cm)	TDS (mg/L)	Ca (mg/L)	Mg (mg/L)	Na (mg/L)	K (mg/L)	SO ₄ (mg/L)	Cl (mg/L)	HCO ₃ (mg/L)	NO ₃ (mg/L)	Br (mg/L)	$\delta^{18}\text{O}$ (‰ vs V-SMOW)	$\delta^2\text{H}$ (‰ vs V-SMOW)	^3H (TU)
1	6	1.85	nd	7.9	15	2.36	1420	95	37.8	372.6	58.11	67.98	552.38	398.04	38.22	3.4	-4.25	-24.28	3.23
2	7	2.95	3.53	nd	nd	nd	nd	nd	nd	nd	nd	nd	nd	nd	nd	nd	nd	nd	nd
3	11.6	11.43	12.07	8.14	19	6.07	3950	134	113.76	949.9	50.31	155.74	1748.73	278.38	6.46	8.9	-4.62	-26.3	1.64
4	9	4.45	5.23	7.98	18.5	1.18	710	92	19.2	128.8	16.38	42.02	217.26	329.22	14.03	7.2	nd	nd	nd
5	4.5	4.3	5.49	8.15	16.5	4.4	2750	101	75.6	745.2	47.58	65.1	1281.55	296.98	9.15	6.8	nd	nd	nd
6	2	1.5	2.4	7.62	22.4	7.9	5150	123	125.88	1350.1	50.7	243.08	2467.25	248	10.98	11	-5.15	-28.9	0.40
7	2	1.02	2.57	nd	nd	nd	nd	nd	nd	nd	nd	nd	nd	nd	nd	nd	nd	nd	nd
8	2.8	2.47	3	8.04	16.9	6.36	4090	133	99.6	1028.1	73.71	201.06	1803.4	350.3	5.31	9.2	-5.24	-30.0	2.04
9	5	0.78	1.33	7.91	17.91	5.36	3490	108	96.6	862.5	27.69	122.78	1623.415	241.18	10.37	8.6	nd	nd	nd
10	nd	nd	nd	7.52	17.52	3.83	2490	103	75.12	554.3	17.94	179.22	1120.735	236.84	15.25	6.8	-5.66	-32.1	0.81
11	nd	nd	nd	7.62	17.62	3.13	2035	212	52.32	273.7	27.69	64.68	863.36	228.78	7.28	5.3	nd	nd	nd
12	9	6.3	9.7	7.41	17.41	2.64	1720	147	47.64	262.2	18.72	77.87	574.745	213.9	12.36	3.4	nd	nd	nd
13	12	4.9	10	7.56	17.2	3.97	2580	273	43.44	441.6	17.16	528.18	858.39	195.3	4.51	5.1	-4.26	-26.9	3.23
14	23	9.73	14.56	7.28	17.2	3.55	2310	205	99.72	289.8	14.82	517.06	679.825	236.84	13.22	3.3	-3.80	-22.4	nd
15	48	33.7	34.45	7.56	18.8	1.78	1160	112	37.8	179.4	13.65	135.55	357.84	326.12	48.8	1.5	-5.21	-29.6	0.55
16	69	49.7	50.1	7.68	20	1.23	800	90	28.2	117.3	9.36	13.6	262.7	298.22	15.26	1	nd	nd	nd
17	80	59.2	61.8	7.91	19.8	1.36	890	95	27.6	140.3	11.7	14.42	317.725	254.2	12.62	1.5	nd	nd	nd
18	37	23	24.5	8.93	20.1	1.55	1020	75	33.36	195.5	15.6	91.05	369.91	110.98	8.91	1.9	nd	nd	nd
19	46	23.9	24.65	nd	nd	nd	nd	nd	nd	nd	nd	nd	nd	nd	nd	nd	nd	nd	nd
20	60	33.4	35.15	7.57	18.5	1.95	1270	103	48.84	220.8	37.05	229.9	349.675	355.88	13.42	1.5	-4.8	-31.2	0.85
21	40	22.97	31.32	7.47	19.5	2.62	1700	169	57.12	223.1	12.09	156.15	560.9	380.68	6.56	2.8	nd	nd	nd
22	28	14.84	21.42	7.94	22	1.47	980	81	38.88	142.6	7.8	82.81	288.26	320.54	7.32	1.2	nd	nd	nd
23	37	21.3	21.9	7.64	22.2	1.38	915	97	33.6	135.7	4.68	62.62	294.65	266.6	45.63	1.2	-5.56	-32.3	1.14
24	29	15.8	17.3	7.74	22.6	1.24	840	70	32.52	131.1	15.21	47.79	252.05	296.36	11.91	0.9	nd	nd	nd
25	25	15.15	16.2	nd	nd	nd	nd	nd	nd	nd	nd	nd	nd	nd	nd	nd	nd	nd	nd
26	25	15.69	17.75	7.52	20.3	1.71	1120	111	35.52	154.1	16.38	64.68	333.7	294.5	9.56	1.3	-5.48	-31.8	0.57
27	35	26.47	30.45	8.04	18.8	1.34	870	75	45.12	149.5	6.63	21.42	318.79	269.08	21.3	1.8	-5.56	-31.8	0.83
28	6.5	6.08	7.1	7.29	21.2	2.44	1585	132	40.2	285.2	8.97	119.89	525.045	463.76	16.56	3	nd	nd	nd
29	9	5.12	6.85	7.25	19.5	3.34	2170	252	67.68	289.8	14.43	272.74	650.36	273.42	21.35	3	nd	nd	nd
30	5	3.26	5.7	7.27	19.9	4.02	2620	273	54.96	432.4	14.04	274.8	780.29	368.28	13.82	3.9	-3.19	-23.4	2.18
31	5	4.35	15.7	7.28	21	3.26	2125	273	27.12	246.1	12.48	229.48	641.13	373.86	11.28	2.8	nd	nd	nd
32	4	2.3	5.8	7.04	19.1	4.3	2780	450	36.48	273.7	17.16	397.17	821.47	342.86	65.21	3.7	-3.67	-25.7	3.15
33	5	2.6	4.5	7.17	19.3	4.14	2690	386	65.04	287.5	5.85	510.05	894.6	314.34	39.32	4.2	nd	nd	nd
34	8	4.38	6.68	7.06	21.2	5.01	3260	433	67.92	409.4	5.07	627.47	1125.35	337.28	28.56	5.2	-4.55	-26.5	3.58

Table 1 continued

Well	Alt. (M.a.s.l)	SL (m/ground surface)	Depth (m/ground surface)	pH	T (°C)	EC (MS/cm)	TDS (mg/L)	Ca (mg/L)	Mg (mg/L)	Na (mg/L)	K (mg/L)	SO ₄ (mg/L)	Cl (mg/L)	HCO ₃ (mg/L)	NO ₃ (mg/L)	Br (mg/L)	δ ¹⁸ O (‰ vs V-SMOW)	δ ³ H (‰ vs V-SMOW)	³ H (TU)	
35	5.5	5.27	7.37	7.1	20	7.5	4875	450	127.92	874	10.14	868.08	1833.93	380.06	68.91	10.1	-4.67	-27.6	3.46	
36	12	5.28	9.48	7.11	20.8	4.4	2860	388	46.32	368	5.07	528.59	975.54	303.18	44.6	5.2	nd	nd	nd	
37	11	9.45	13.34	7.14	22.1	4.06	2640	236	83.28	460	62.01	180.46	1073.52	345.34	21.52	5.9	nd	nd	nd	
38	24	7.75	25.6	7.07	20.2	5.04	3275	392	57.6	533.6	16.77	573.5	1241.08	354.64	12.28	5.9	-4.53	-28.0	5.09	
39	9	5.7	10.2	7.23	19.5	4.7	3055	354	55.68	529	35.88	391.4	1106.89	317.44	18.31	5.7	-4.92	-28.8	1.13	
40	12	3.25	7.75	7.7	21.1	5.56	3648	500	70.08	531.3	25.35	742.01	1158.01	309.38	43.56	5.6	nd	nd	nd	
41	7	2.66	6.03	7.12	19.3	5.98	3880	377	84.48	772.8	40.95	621.29	1393.02	347.82	76.31	6.7	nd	nd	nd	
42	5	0.54	5.35	8.72	20.7	3.4	2210	138	70.32	538.2	26.91	253.67	842.06	367.04	51.5	4.7	nd	nd	nd	
43	7	4.1	8.82	7.43	19.6	5.23	3400	305	67.2	724.5	28.08	697.1	1183.57	419.74	40.93	5.7	-4.18	-26.3	3.65	
44	38	3.42	12.12	7.47	19.8	5.21	3390	264	37.68	814.2	7.8	745.72	1118.96	470.58	26.12	5.6	-3.45	-22.7	3.25	
45	8	4.1	6.9	7.24	20.8	4.27	2775	316	31.92	496.8	15.6	446.19	986.9	332.94	136.01	5.1	nd	nd	nd	
46	3	0.53	5.93	7.84	18.7	6.4	4160	356	61.92	908.5	16.77	697.1	1629.45	365.8	102.21	8	-4.19	-23.6	3.36	
47	10	6.82	12.14	7.35	20.6	5.01	3257	374	38.4	627.9	40.95	615.53	1168.66	304.42	26.05	6	-4.62	-27.7	2.81	
48	7	3.9	6.7	7.3	19.2	3.6	2340	270	5.28	439.3	39.78	363.79	704.32	363.94	56.18	3.3	-4.65	-28.4	2.76	
49	15	7.95	12.2	7.06	20.3	3.78	2450	335	24.96	365.7	12.48	232.78	874.01	295.12	41.31	4.3	nd	nd	nd	
50	32	11.99	14.45	7.09	21.5	2.98	1940	264	16.08	243.8	9.36	124.42	681.6	296.98	6.28	3	-4.75	-29.1	4.07	
51	3	2.08	5.95	7.18	19.5	3.93	2550	348	26.64	372.6	16.77	237.72	881.82	284.58	86.41	4	-4.74	-28.7	3.91	
52	14	9.25	13.35	7.41	20.5	3.35	2180	278	44.16	361.1	16.77	289.63	724.91	249.86	21.62	3	nd	nd	nd	
53	3	1.4	4.66	7.15	19.9	3.11	2030	256	17.76	276	17.16	166.04	695.09	319.92	51.83	3.1	nd	nd	nd	
54	33	21.3	22.14	7.4	22	2.06	1240	175	34.32	186.3	62.01	27.6	418.9	269.08	8.72	1.6	-5.26	-31.9	2.97	
55	11	5.8	9	7.41	18.9	3.68	2210	296	61.68	365.7	8.97	356.38	838.51	355.88	43.28	4.4	-4.08	-24.7	3.81	
56	26	13.9	15.8	7.33	22.1	2.36	1420	164	58.32	213.9	7.41	119.89	556.64	312.48	29.19	2.3	nd	nd	nd	
57	9	8.12	10.67	7.32	21	2.2	1320	182	37.44	246.1	30.03	81.99	482.8	373.24	36.14	1.9	-4.66	-29.4	4.56	
58	35	14.05	22	7.52	21	1.82	1100	105	55.68	220.8	19.89	95.17	402.57	353.4	10.16	1.3	-5.06	-31.4	2.76	
59	10	5.48	8.05	7.27	21.4	4.53	2730	203	65.52	621	6.63	241.43	1160.85	407.96	25.12	6.1	nd	nd	nd	
60	12	5.33	7.23	7.4	20	1.64	980	170	2.4	128.8	3.51	117.01	260.57	328.6	10.85	0.8	-4.98	-30.6	3.12	
61	21	9.6	15.6	nd	nd	nd	nd	nd	nd	nd	nd	nd	nd	nd	nd	nd	nd	nd	nd	nd
62	nd	nd	nd	7.4	19.9	2.17	1300	131	59.76	236.9	11.31	60.15	446.59	393.08	42.36	1.9	-4.95	-30.3	2.39	nd
63	19	6.21	9.21	nd	nd	nd	nd	nd	nd	nd	nd	nd	nd	nd	nd	nd	nd	nd	nd	nd
64	22	8.65	11.3	7.36	21.1	1.36	810	106	37.44	135.7	5.85	17.72	274.06	330.46	36.41	0.9	nd	nd	nd	nd
65	4	2.55	10.9	nd	nd	nd	nd	nd	nd	nd	nd	nd	nd	nd	nd	nd	-5.4	-30.5	3.74	nd
66	52	13.78	26.55	7.05	21.7	3.25	1950	266	25.68	246.1	11.31	37.9	834.25	391.84	39.18	3.8	-2.97	-19.1	1.43	nd
67	50	11.2	50.9	nd	nd	nd	nd	nd	nd	nd	nd	nd	nd	nd	nd	nd	nd	nd	nd	nd
68	59	8.45	nd	nd	nd	nd	nd	nd	nd	nd	nd	nd	nd	nd	nd	nd	nd	nd	nd	nd

Table 1 continued

Well	Alt. (M.a.s.l)	SL (m/ground surface)	Depth (m/ground surface)	pH	T (°C)	EC (MS/cm)	TDS (mg/L)	Ca (mg/L)	Mg (mg/L)	Na (mg/L)	K (mg/L)	SO ₄ (mg/L)	Cl (mg/L)	HCO ₃ (mg/L)	NO ₃ (mg/L)	Br (mg/L)	δ ¹⁸ O (‰ vs V-SMOW)	δ ² H (‰ vs V-SMOW)	³ H (TU)
69	nd	nd	nd	8.23	22.8	3.75	2250	151	84.48	535.9	7.8	173.04	999.68	251.1	26.36	5.2	-5.36	-31.9	3.34
70	39	5.42	nd	nd	nd	nd	nd	nd	nd	nd	nd	nd	nd	nd	nd	nd	nd	nd	nd
LW				7.83		40.5	32,400	420	1368	9376	366	2755	16788	126	0.05	68.35			
SW				7.86		40.1	32,160	418	1356	9325	374	2776	16,979	122	0.07	68.16			

Alt. altitude, SL static level, LW lagoon water, SW sea water

In the study area, vegetable cropping systems under intensive irrigation are the main agriculture activities. However, arboriculture and grain farming predominated in the foothills area. Around the most important villages (Gournata, Ezzouaouine, Oussja, and Ghar el Melah), cultivated areas are sometimes greatly reduced by increasing urbanization of local agglomerations. This expansion of urban areas is due to an increase in the local population and the suburbanization phenomenon around the capital Tunis. Due to this changing the pressure on water resources in the study area has increased dramatically in recent decades because of the extension of agricultural and urban lands. This has led to a deterioration of water quality.

The important salinity of the groundwater observed in the central part of the plain and around Oussja and the Ghar el Melah lagoon (Fig. 5) is the consequence of multiple phenomena:

- The first one is related to aquifer lithology that changes from a sandy one in the upper stream part of the basin to a most clayey and silty one in the lower part of the plain.
- The second one is the return of irrigation water to the aquifer that characterizes the lower part of the plain intensively cultivated and where the water table levels are less than 10 m. Indeed, in semi-arid regions, intensive irrigation by groundwater causes recycling of salts accumulated in surface and their transfer through the unsaturated zone and their accumulation in the aquifer: salts accumulated in the soil during dry periods are flushed to the aquifer during rainy season. Figure 7a clearly shows that the shallower horizons (depth ≤ 10 m) present the highest values of EC. Excess irrigation water return flow to the aquifer is confirmed also by high NO₃⁻ contents characterizing the shallowest levels (depth ≤ 10 m). This contamination comes certainly from the surface by return of irrigation water or/and by the precipitation as highlighted in Fig. 7b.
- The third one is the effect of marine sprays. In coastal areas, salts resulting from marine sprays are accumulated on the surface and then recycled by precipitation or by irrigation water to the aquifer (Cruz and Silva 2000). This is clearly illustrated by the evolution of the Cl⁻ and Br⁻ concentrations versus the depth of the water table (Fig. 8).

Major elements geochemistry

Considering the ion concentrations, a classification into two groundwater types was made of the 61 samples collected in the area: Cl⁻-Na⁺ and Cl⁻-Na⁺/Ca²⁺ type. The

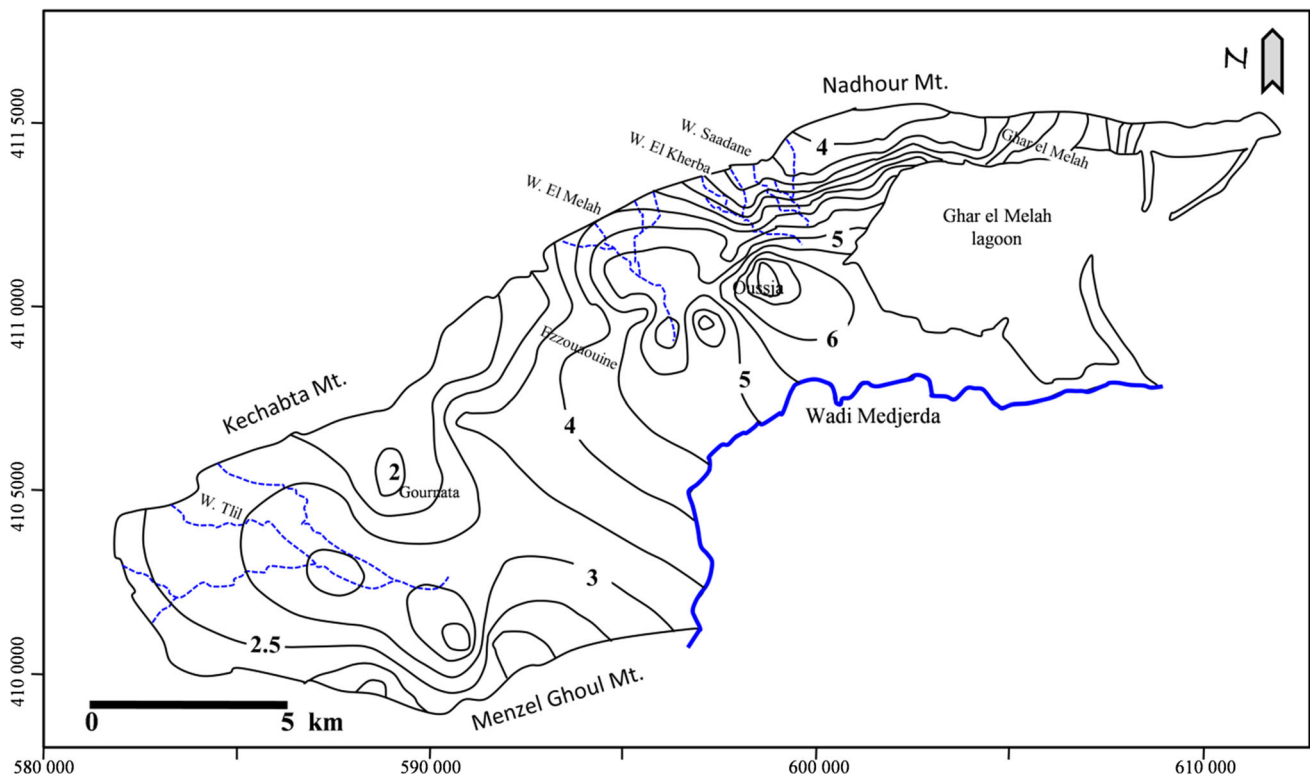


Fig. 5 Electric conductivity (mS/cm) contour map

Table 2 Correlation matrix of TDS and chemical elements in groundwater

	TDS	Ca ²⁺	Mg ²⁺	Na ⁺	K ⁺	SO ₄ ²⁻	Cl ⁻	HCO ₃ ⁻	NO ₃ ⁻	Br ⁻
TDS	1.00									
Ca ²⁺	0.61	1.00								
Mg ²⁺	0.67	0.08	1.00							
Na ⁺	0.91	0.26	0.72	1.00						
K ⁺	0.34	-0.10	0.34	0.48	1.00					
SO ₄ ²⁻	0.72	0.81	0.33	0.50	-0.04	1.00				
Cl ⁻	0.96	0.41	0.74	0.96	0.41	0.54	1.00			
HCO ₃ ⁻	0.13	0.22	-0.06	0.12	-0.01	0.25	0.05	1.00		
NO ₃ ⁻	0.28	0.49	-0.06	0.16	-0.12	0.42	0.18	0.28	1.00	
Br ⁻	0.88	0.34	0.70	0.90	0.40	0.49	0.93	0.04	0.14	1.00

Cl⁻-Na⁺ type dominates the low part of the plain, whereas the Cl⁻-Na⁺/Ca²⁺ type characterizes the upstream and the NW parts (except wells number 58, 59 and 69).

As shown in the Table 2 a well-defined correlations characterize the relationship of the TDS values and Na⁺ and Cl⁻ contents (respective $r^2 = 0.91$ and 0.96). These correlations indicate that the inferred elements are the major contributor to the groundwater mineralization.

The Na⁺/Cl⁻ relationship (Fig. 9) shows that this two elements are strongly correlated ($r^2 = 0.91$) and that the low Na⁺/Cl⁻ ratio (0.78) closely approach sea and lagoon water values (respectively, 0.85 and 0.86) and typical

seawater value (0.86) (Vengosh et al. 1999; Fedrigoni et al. 2001). In the current state of knowledge, there is no seawater intrusion detected by hydrodynamic measurements (Fig. 3), so high Cl⁻ values can be attributed to the effect of marine sprays and halite dissolution. Indeed, in the semi-arid regions, salts accumulated on ground surface by evaporation of meteoric water, irrigation water and marine sprays, are dissolved in the next rainy event and flushed to the aquifer. This phenomenon characterizes especially the lower area of the plain near the coast wherein lowest depths of the water table and highest Cl⁻ contents (500–2500 mg/L) were measured.

Fig. 6 Piper diagram of groundwater. LW lagoon water, SW sea water

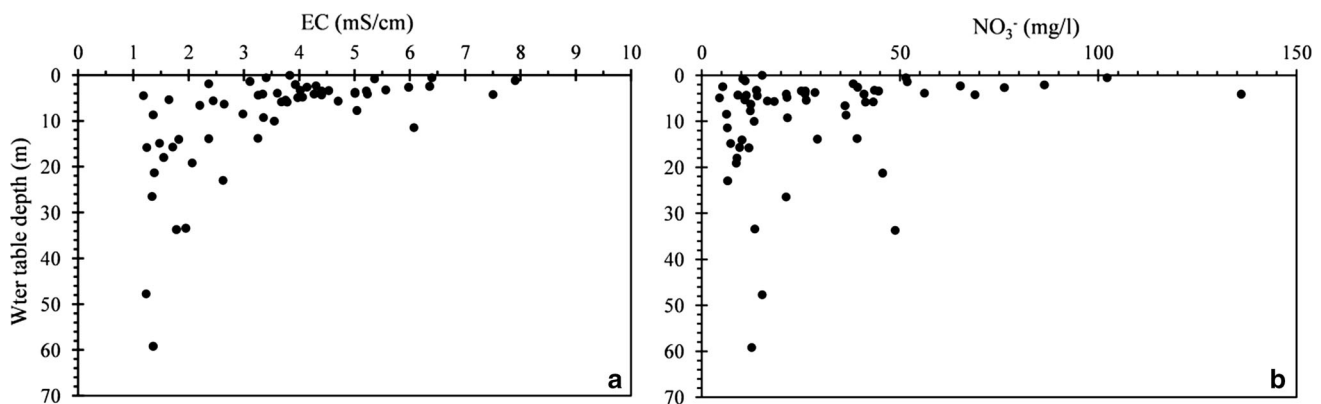
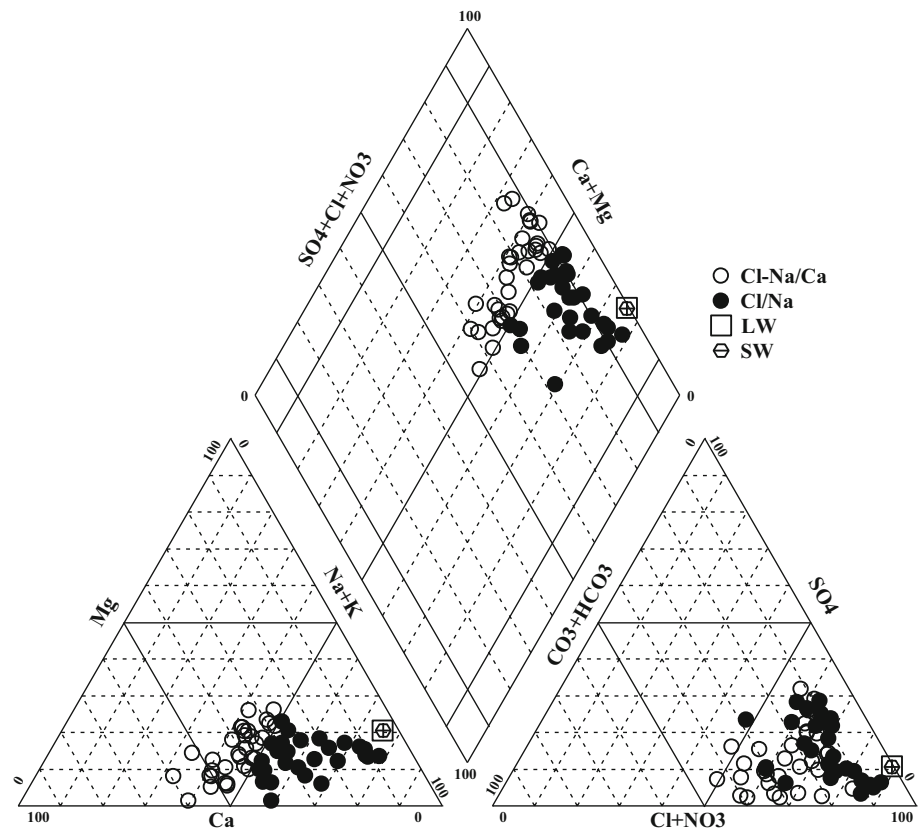


Fig. 7 Evolution of EC values (a) and NO_3^- contents (b) with water table depth

In addition, the observed general decreasing trend in Na with increasing in Cl^- ($\text{Na}^+/\text{Cl}^- < 1$) along the flow direction could be due to ion-exchange process. The hypothesis of cation exchange that affects groundwater is showed by the $\text{Ca}^{2+} + \text{Mg}^{2+} - \text{SO}_4^{2-} + \text{HCO}_3^-$ relationship in Fig. 10. During the cation exchange process clay particles of the aquifer exchange Ca^{2+} and Mg^{2+} against Na^+ . This process implies a decrease of Na^+ in the groundwater against an increase in Ca^{2+} and Mg^{2+} (Appelo and Postma 1994; Hem 1992). If the cation exchange is the only process controlling the composition

of groundwater, the relation between $\text{Ca}^{2+} + \text{Mg}^{2+}$ and $\text{SO}_4^{2-} + \text{HCO}_3^-$ should be linear with a slope of 1 (Vengosh et al. 1999). The Fig. 10 shows that the Ca^{2+} and Mg^{2+} are in excess with respect to $\text{SO}_4^{2-} + \text{HCO}_3^-$. This can be explained by the dissolution of carbonate (calcite, dolomite and aragonite) and evaporate mineral (gypsum and anhydrite). Indeed the saturation indexes (SI) of dissolved minerals revealed that the groundwater is generally saturated in carbonate minerals (calcite, aragonite and dolomite) and undersaturated with respect to gypsum and anhydrite.

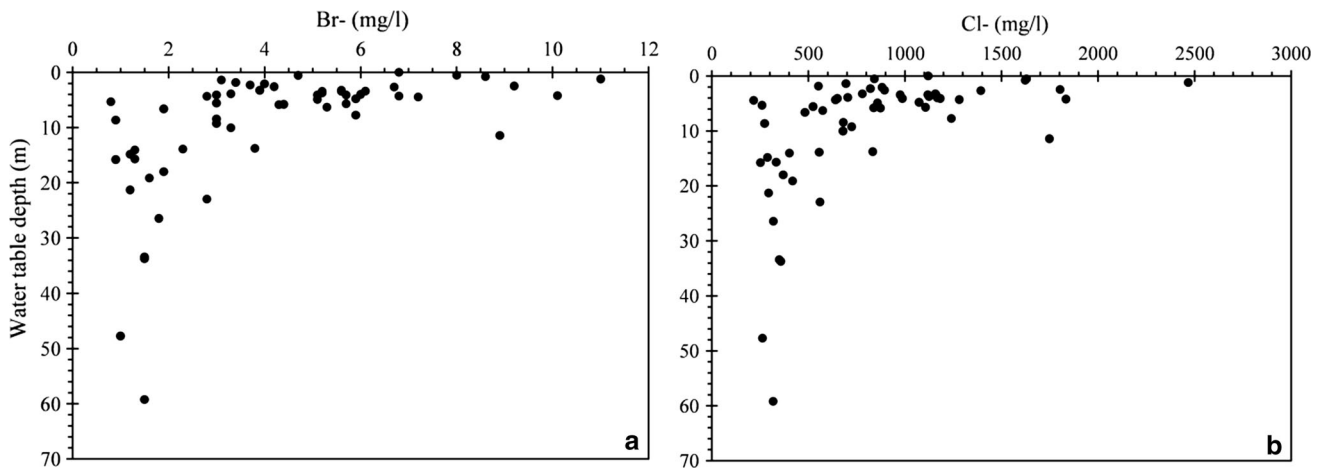


Fig. 8 Bromide (a) and chloride (b) concentrations vs depth

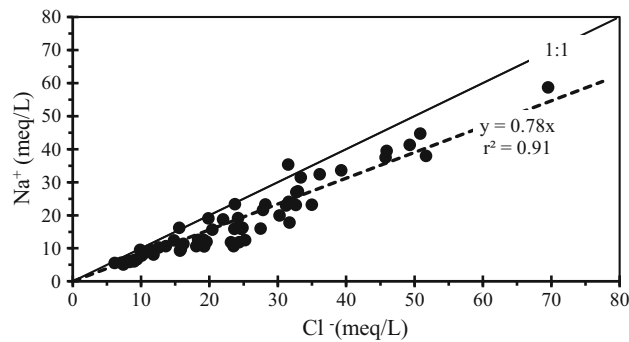


Fig. 9 Cl^- vs Na^+ concentrations in the groundwater

Br^-/Cl^- relationship

In natural water, Br^- and Cl^- are considered conservative tracers and the Br^-/Cl^- ratio is not influenced by base-exchange reaction (Vengosh et al. 1999; Fedrigoni et al. 2001, Knuth et al. 1990; David and William 1997; Freeman 2007). This characteristic has led to the use of Br^- concentrations and Br^-/Cl^- mass ratios to infer the geochemical provenance of different groundwater (e.g., dissolution of halite or sea intrusion) in coastal areas.

In the plain of OGM, bromide concentrations in groundwater are relatively high, mostly near the coast and around the lagoon of Ghar el Melah. Br^- contents vary from 0.8 mg/L in NW part of the plain to 11 mg/L in the coastal region situated east of Ghar el Melah. Bromide concentrations show the same trend as the chloride against water table depth (Fig. 8) indicating their marine origin due to marine sprays. In Fig. 11, Br^- and Cl^- contents show good correlation ($r^2 = 0.97$) and Br^-/Cl^- ratio is constant (2.2 ‰) and is slightly higher than that of Mediterranean water (1.5 ‰) defined by Vengosh et al. (1999). High Br^-/Cl^- ratio in groundwater observed in the vicinity of the coast can be

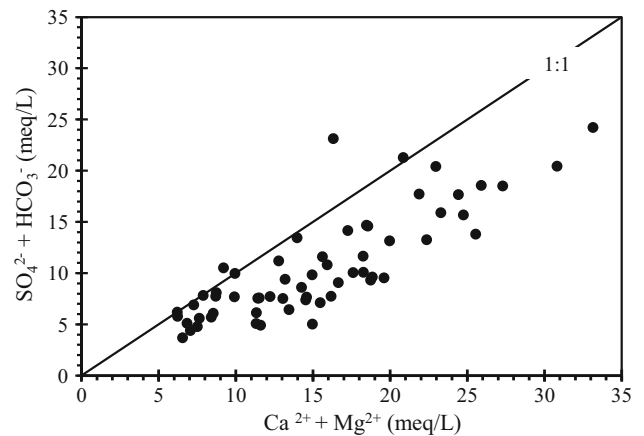


Fig. 10 Relation between $\text{Ca}^{2+} + \text{Mg}^{2+}$ and $\text{SO}_4^{2-} + \text{HCO}_3^-$ in the study area

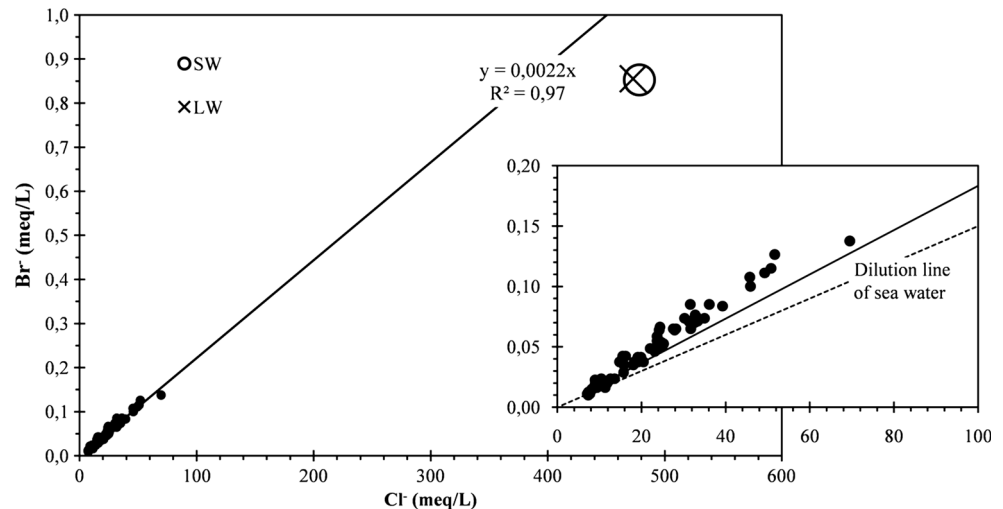
explained by the leaching of salts (derived from marine sprays) deposited on the ground, by rainwater and irrigation water. Similar findings are reported by Vengosh et al. (1999) in the Mediterranean basin.

Groundwater sampled in wells situated away from the coast and the Ghar el Melah lagoon in the upstream part of the plain and in the southwest part of the plain, present Br^-/Cl^- ratios close to 1.5 ‰ (marine ratio). This suggests a primary source for chloride and bromide related to salts formed on the surface and driving from sea sprays. Salts accumulated on the ground surface are then dissolved and flushed to the aquifer by rain water.

Nitrate concentration in groundwater

Nitrate is the most common water contaminant index for anthropogenic sources (Freeze and Cherry 1979). Irrigation and fertilizer use can have profound impact on the

Fig. 11 Relation between chloride and bromide in the groundwater, sea water and lagoon water



hydrology and quality of water resources in agricultural regions (Johnston et al. 1998; Gourcy et al. 2009). Excessive infiltration of irrigation water can introduce agriculture contaminants (e.g. nitrate) to shallow groundwater, increase recharge rates and significantly alter groundwater residence times (Böhlke 2002). Nitrate pollution of groundwater may stem from different sources, including fertilizers, animal waste and domestic and industrial discharge. The use of fertilizers in farming areas is, however, considered to be the main source of NO_3^- groundwater contamination (Hill 1982; Grassi et al. 2007).

In the study area, synthetic fertilizers and waste animals are largely used by farmers. In the absence of system of wastewater treatment, domestic water is discharged directly into individual septic tanks. As shown in Fig. 7b, the most contaminated horizons are the shallowest levels (depth <10 m), which are characterized by NO_3^- contents of up to about 140 mg/L. The most contaminated area is the lower part of the plain between Ezzouaouine and Oussja where NO_3^- values range between 50 and 136 mg/L. In this part of OGM plain agriculture activities are more developed (Fig. 12).

In the upstream part of the basin and in the region situated in the eastern part of Ghar el Melah city, no recharge by water irrigation return was observed and the NO_3^- values are less than 40 mg/L and ion concentration decreased as the well depth increased. This is related to the important depth of the water table and to agriculture practices (arboriculture).

Isotope study

In arid and semi-arid regions, groundwater recharge occurs subsequent to heavy and long-term precipitations characterizing the humid season. The short-term precipitations

with small amounts do not contribute to groundwater recharge as evaporation exceeds infiltration rates. To understand the relationship between isotopic composition of groundwater and those of precipitation as input function, we refer to values measured at the station of Tunis situated at 30 km in the south from the plain of Oussja Ghar el Melah for both stable isotopes (^{18}O and ^2H) and tritium. Stable isotope values in this station for ^{18}O and ^2H , respectively, are -4.5 and 25.1 ‰ in the rainy season and -1.1 and -1.2 ‰, respectively, in the dry season (Celle-Jeanton et al. 2001). Local meteoric water line (LMWL) was defined by Celle-Jeanton et al. (2001) as: $\delta^2\text{H} = 8\delta^{18}\text{O} + 11$. Then, groundwater with a $\delta^2\text{H}/\delta^{18}\text{O}$ slope of ≈ 8 may indicates origin from meteoric water with minimal past-precipitation effects, whereas a slope <8 may reflects evaporation during or after rainfall and/or mixing with an external water source with high $\delta^{18}\text{O}$ and $\delta^2\text{H}$ values (e.g., return of irrigation water). Tritium content of the rain water in recent years shows an annual natural level ranging between 5 and 10 TU (IAEA 1995; IAEA/GNIP).

Thirty four groundwater samples were analyzed for the isotope study. The results show isotopic content ranging from -5.66 to -2.97 ‰ vs V-SMOW for $\delta^{18}\text{O}$ and from -32.3 to -19.1 ‰ vs V-SMOW for $\delta^2\text{H}$. The mean values are, respectively, -4.66 and -28.1 ‰ vs V-SMOW for $\delta^{18}\text{O}$ and $\delta^2\text{H}$ (Fig. 13). The average values of stable isotopes are similar to those of precipitations in the humid season suggesting that the groundwater derived from rainfall origin. However, in the detail groundwater isotopic composition varies into different groups according to geographical location in the plain, well depth and recharge mode.

An evaporative effect in stable isotopes is seen for groundwater sampled in the low part of the plain and around the village of Oussja. In these areas, isotope values

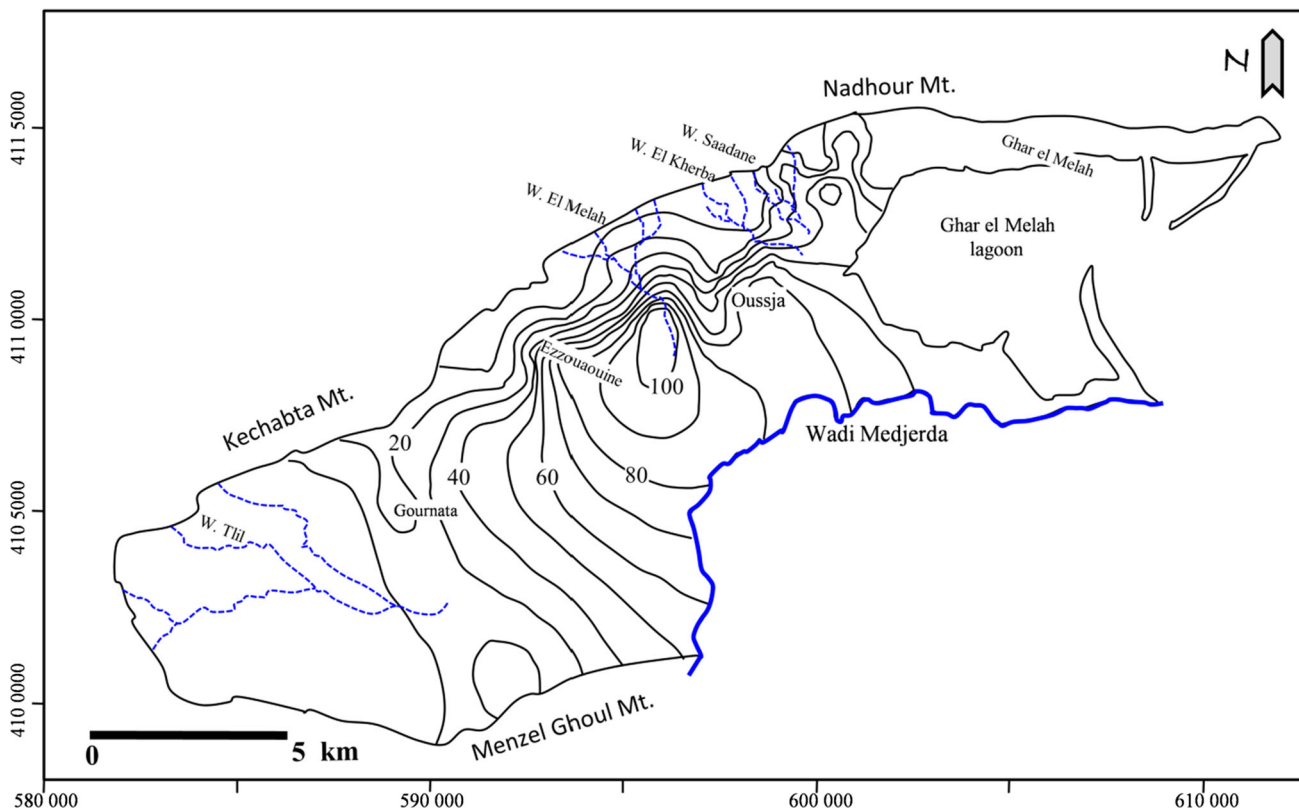


Fig. 12 NO₃⁻ distribution map in the OGM plain

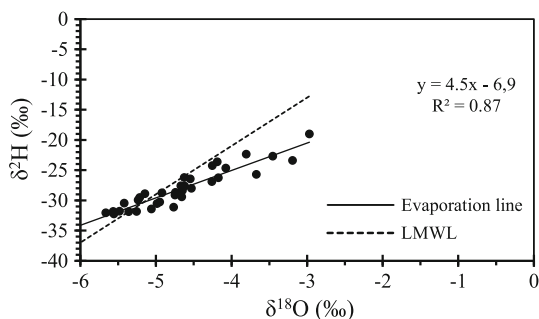


Fig. 13 Plot of δ²H vs δ¹⁸O for the groundwater

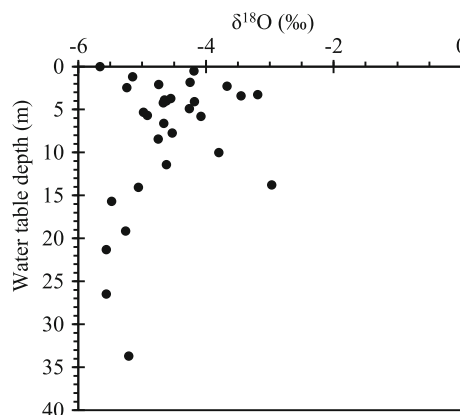


Fig. 14 Evolution of δ¹⁸O with water table depth

within 10 m (Fig. 14) below the ground fall on the evaporation line ($\delta^2\text{H} = 4.5\delta^{18}\text{O} - 6.9$) indicating possible surface water contribution (irrigation water) to the aquifer. Isotope composition show enriched values varying between -4.26 and -2.97 ‰ for ¹⁸O, and between -26.9 and -19.1 ‰ for ²H. The evaporative effect could also be due to near-surface evaporation in the unsaturated zone during natural recharge for some samples. Isotope findings are corroborated by similar observations for EC, Cl⁻, Br⁻ and NO₃⁻ (Figs. 7, 8). The Tritium content of this type of water ranges between 1.43 and 3.81 TU indicating some

modern recharge component probably between 1950 and 1980.

A second group of more depleted values of stable isotopes ranging between -5.66 and -5.15 ‰ for ¹⁸O and between -32.3 and -28.9 ‰ for ²H characterizes groundwater from the upstream part of the plain (well 15, 23, 26, 27), the region situated in the East of the village of Ghar el Melah (well 3, 6, 8 and 10) and the western part of

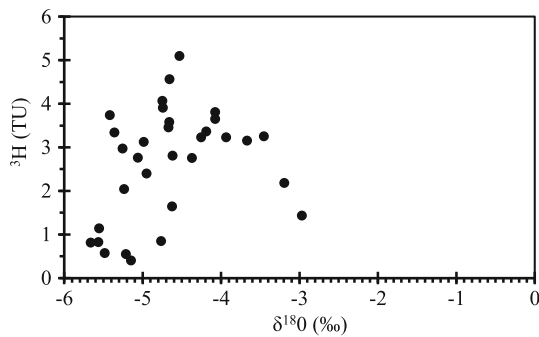


Fig. 15 Plot of ^3H contents vs $\delta^{18}\text{O}$ for the groundwater

the basin (well 39, 54, 65, 69). On the $^{18}\text{O}/^2\text{H}$ graph (Fig. 13), representative points of this type of water lie on and around the LMWL with a deuterium excess (d) values in the range of 10.2 to 13.2 ‰ indicating rapid recharge and a lack of evaporation effect prior to infiltration and reflecting groundwater replenishment under more humid

climatic conditions during earlier times around 1950 or older. In fact tritium content of this type of groundwater is below 1 TU (Fig. 15). Carbon-14 dating is needed to confirm the age of this type of groundwater.

An intermediate isotope composition between the two previous groups and similar to that of the local meteoric water based on present-day precipitations is observed in the middle part of the plain between Oussja and Gournata and its southern part around the Wadi TliI. Stable isotopes are between -5 and -4 ‰ for ^{18}O and from -32 to -27.0 ‰ for ^2H with modern-day ^3H levels ranging from 1.6 to over 5 TU (Fig. 15). The highest tritium values (between 4 and 5 TU) measured in central part of the plain between Oussja and Gournata (well 38, 50, 51, and 57) reflect recent recharge (posterior to 1980) by rapid infiltration of rainwater. Tritium content of rain water measured in Tunis and Sfax (situated, respectively, at 50 and 300 km in the south), was about 6.2 and 5.33 TU in 1997 (IAEA/GNIP).

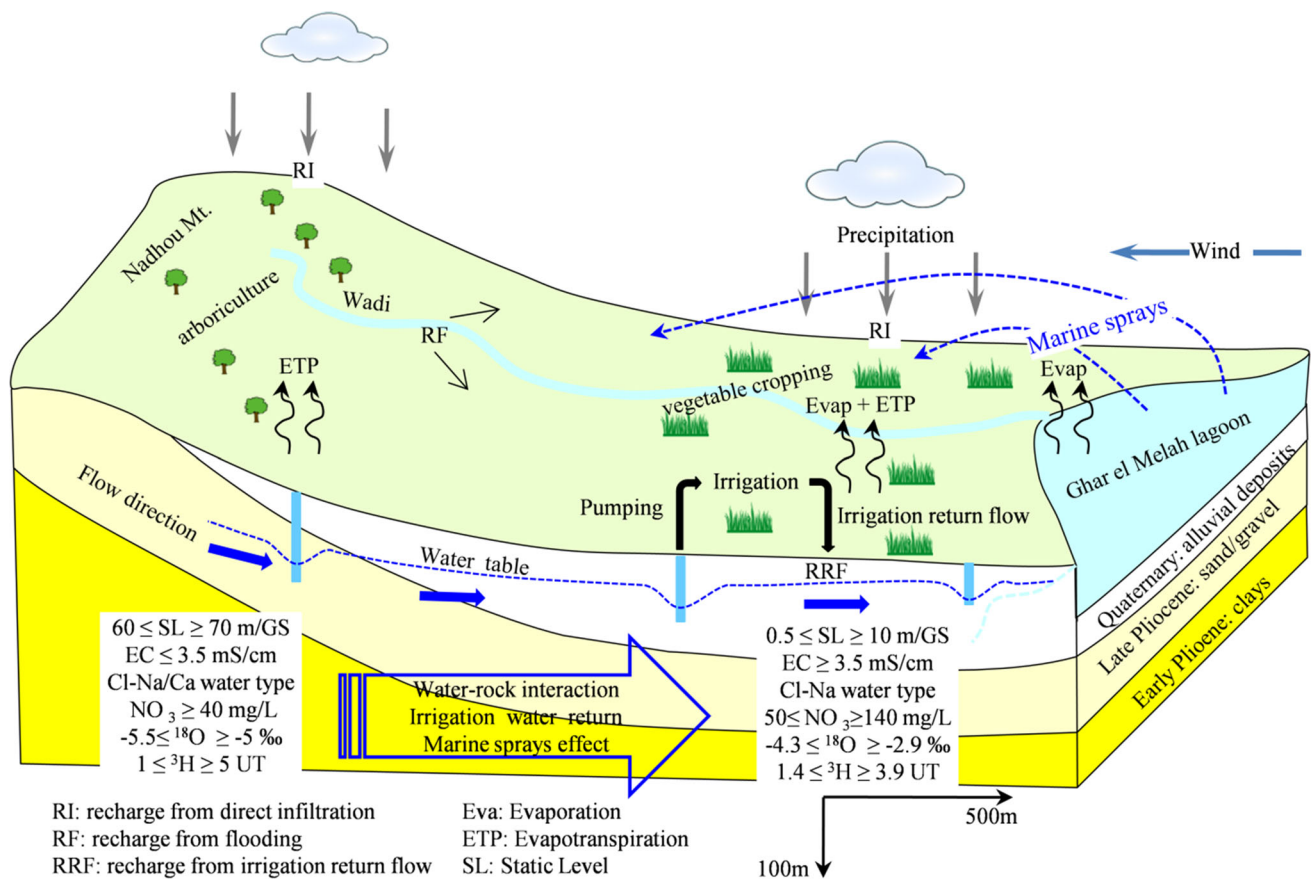


Fig. 16 Schematic conceptual model summarizing groundwater flow, geochemical and isotopic evolution and salinization sources of groundwater in the NE part of the OGM plain

Conclusion

This study investigated the salinization processes and degradation of the groundwater in the shallow coastal aquifer of Oussja Ghar el Melah using a dual geochemical and isotopic approach. Results of this investigation are expected to represent general conditions in many other coastal Tunisian and Mediterranean aquifers suffering joint hard natural conditions and severe anthropic constraints.

Based on different geochemical parameters (e.g. EC, Cl^- , Br^- , NO_3^- , Na^+/Cl^- and Br^-/Cl^- ratios) and well characteristics (e.g., depth and location) different water types were distinguished and many sources of groundwater salinization were highlighted. Mineral saturation states and ionic relations indicate that the major geochemical process controlling hydrochemical evolution are dissolution of soil salts, dissolution to saturation of carbonate minerals, dissolution of gypsum and halite and cation exchange. In addition, in many area in the plain, the marine sprays accumulated as a salts on the surface and then leached and flushed to the aquifer by rainwater or return of irrigation water constitute a primary source of groundwater salinization. In the central and lower part of the plain where the water table levels are less than 10 m and agriculture activities are the most intense high concentration of nitrate were measured. Nitrates derived from fertilizers intensively used by farmers are transported to the aquifer by natural recharge process and by return flow from irrigation water (Fig. 16).

Hydrochemical observations are confirmed by isotopic study. Stable isotope signature and tritium contents of groundwater provide evidence for recent groundwater recharge by infiltration of local precipitations and return flow from irrigation. Low tritium values with depleted ^{18}O and ^2H in some areas of the plain suggest more earlier recharge (pre-nuclear period) that occurs probably under different climate conditions.

Finally, authorities charged for water management must take urgent necessary measures in the aim to encourage more rational use of fertilizers and to reduce the use of groundwater in irrigation to prevent seawater intrusion. If seawater intrusion takes place the restoration of the aquifer may take a very long time. For example, Appelo and Postma (1994) estimate about 40 years to refresh 2 m thick in the case of seawater intrusion.

References

- Appelo CAJ, Postma D (1994) Geochemistry, groundwater and pollution. Balkema, Rotterdam
- Barale V, Folving S (1996) Remote sensing of coastal interactions in the Mediterranean region. *Ocean Coast Manag* 30:217–233
- Böhlke JK (2002) Groundwater recharge and agricultural contamination. *Hydrogeol J* 10:153–179
- Burrolet PF, Dumon E (1952) Geological map of Porto Farina. ONM, Tunisia
- Celle-Jeanton H, Zouari K, Travi Y, Daoud A (2001) Isotopic characterisation of the precipitation in Tunisia. Variations of the stable isotope compositions of rainfall events related to the origin of air masses. *C R Acad Sci* 333:625–631
- Chelbi F, Paskoff R, Troussset P (1995) La baie d'Utique et son évolution depuis l'Antiquité: une réévaluation géoarchéologique. In: *Antiquités africaines*, 31, pp 7–51
- Clark I, Fritz P (1997) Environmental isotopes in hydrogeology. CRC Press, Boca Raton
- Cruz JV, Silva MO (2000) Groundwater salinization in Pico Island (Azores, Portugal): origin and mechanisms. *Environ Geol* 39(10):1181–1189
- Custodio E (2010) Coastal aquifers of Europe: an overview. *Hydrogeol J* 18(1):269–280. doi:10.1007/s10040-009-0496-1
- Custodio E, Bruggeman KA (1987) Groundwater problems in coastal areas, UNESCO. *Stud Repo Hydrol* 45:596
- David CA, William BF (1997) Use of bromide:chloride ratios to differentiate potential sources of chloride in a shallow, unconfined aquifer affected by brackish-water intrusion. *Hydrogeol J* 5(2):17–26
- Fedrigoni L, Krimissa M, Zouari K, Maliki A, Zuppi GM (2001) Origine de la minéralisation et comportement hydrogéochimique d'une nappe phréatique soumise à des contraintes naturelles et anthropiques sévères: exemple de la nappe de Djebeniana (Tunisie). *C R Acad Sci* 332:665–671
- Freeman JT (2007) The use of bromide and chloride mass ratios to differentiate salt-dissolution and formation brines in shallow groundwaters of the western Canadian sedimentary basin. *Hydrogeol J* 15:1377–1385
- Freeze RA, Cherry JA (1979) Groundwater. Prentice Hall, Englewood Cliffs, p 604
- Fukada T, Hiscock KM, Dennis PF (2004) A dual-isotope approach to the nitrogen hydrochemistry of an urban aquifer. *Appl Geochem* 19:709–719
- Gourcy L, Baran N, Vittecoq B (2009) Improving the knowledge of pesticide and nitrate transfer processes using age-dating tools (CFC, SF, H) in a volcanic island (Martinique, French West Indies). *J Contam Hydrol* 108:107–117
- Grassi S, Corceci G (2005) Hydrogeology and geochemistry of the multilayered confined aquifer of the Pisa Plain (Tuscany–Central Italy). *Appl Geochem* 20:41–54
- Grassi S, Corceci G, Squarci P (2007) Groundwater resource degradation in coastal plains: the example of the Cecina area (Tuscany–Central Italy). *Appl Geochem* 22:2273–2289
- Hem JD (1992) Study and interpretation of the chemical characteristics of natural water (3rd ed): US Geological Survey Water Supply. Paper, 2254, p 263
- Hill AR (1982) Nitrate distribution in the groundwater at the Alliston region of Ontario, Canada. *Ground Water* 20:696–702
- IAEA (1995) Reference and intercomparison materials for stable isotopes of light elements. In: *Proceedings of a consultants meeting held in Vienna, 1–3/10/1993*, IAEA, Vienna, TECDOC-825, p 165
- IAEA/GNIP data. http://www-naweb.iaea.org/naweb/ih/IHS_resources_gnip.html
- Johnston CT, Cook PG, Frappe SK, Plummer LN, Busenberg E, Blackport RJ (1998) Ground water age and nitrate distribution within a glacial aquifer beneath a thick unsaturated zone. *Ground Water* 36:171–180

- Kass A, Gavrieli I, Echieli Y, Vengosh A, Starinsky A (2005) The impact of freshwater and wastewater irrigation on the chemistry of shallow groundwater: a case study from the Israeli coastal aquifer. *J Hydrol* 300:314–331
- Knuth M, Jackson JL, Whittemore DO (1990) An integrated approach to identifying the salinity source contaminating a groundwater supply. *Ground Water* 28:207–214
- Kouzana L, Ben Mammou A, Sfar Felfoul M (2009) Seawater intrusion and associated processes: case of the Korba aquifer (Cap-Bon, Tunisia). *C R Geosci* 341:21–35
- Ma F, Yang YS, Yuan R, Cai S Z, Pan S (2007) Study of shallow groundwater quality evolution under saline intrusion with environmental isotopes and geochemistry. *Environ Geol* 51:1009–1017
- Mejri L (2012) Tectonique quaternaire, paléosismicité et sources sismogéniques en Tunisie nord-orientale: Etude de la faille d'Utique. PhD Thesis: Univ. Toulouse, p 184
- Mejri L, Regard V, Carretier S, Brusset S, Dlala M (2010) Evidence of Quaternary active folding near Utique (Northeast Tunisia) from tectonic observations and a seismic profile. *C R Geosci* 342:864–872
- Melki F, Zouaghi T, Harrab S, Casas Sainz A, Bedir M, Zargouni F (2011) Structuring and evolution of Neogene transcurrent basins in the Tellian foreland domain, north-eastern Tunisia. *J Geodyn* 52:57–69
- Oueslati A, Charfi F, Baccar F (2006) Presentation of the tunisian site: la basse vallée de oued Mejerda et la lagune de Ghar el Melah. Fifth International Meeting INCO-CT-2005-015226, p 26
- Re V, Zuppi GM (2011) Influence of precipitation and deep saline groundwater on the hydrological systems of Mediterranean coastal plains: a general overview. *Hydrol Sci J* 56(6):966–980
- Stigter TY, Van Ooijen SPJ, Post VEA, Appelo CAJ, Carvalho Dill AMM (1998) A hydrogeological and hydrochemical explanation of the groundwater composition under irrigated land in a Mediterranean environment, Algarve, Portugal. *J Hydrol* 208:262–279
- Trabelsi R, Zairi M, Ben Dhia H (2007) Groundwater salinization of the Sfax superficial aquifer, Tunisia. *Hydrogeol J* 15:1341–1355
- Vengosh A, Spivack AJ, Artzi Y, Ayalon A (1999) Geochemical and Boron, strontium and oxygen isotopic and geochemical constraints for the origin of the salinity in groundwater from the Mediterranean coast of Israel. *Water Resour Res* 35:1877–1894